Malaysian Journal of Analytical Sciences (MJAS)



Published by Malaysian Analytical Sciences Society

HARNESSING OF PEANUT SHELL WASTE-DERIVED ACTIVATED CARBON FOR EFFICIENT MAGNETIC SOLID PHASE EXTRACTION OF CALCIUM CHANNEL BLOCKERS DRUGS FROM WATER

(Memanfaatkan Karbon Teraktif dari Sisa Kulit Kacang Tanah untuk Pengekstrakan Fasa Pepejal Magnetik yang Berkesan terhadap Dadah Penyekat Saluran Kalsium daripada Air)

Fatin Nur Umirah Sukardan¹, Farahdina Man², Usman Armayau^{1,3}, Saw Hong Loh¹, Marinah Mohd Ariffin¹, and Wan Mohd Afiq Wan Mohd Khalik^{1,4}

¹Faculty of Science and Marine Environment, Universiti Malaysia Terengganu, 21030 Kuala Nerus, Malaysia ²Biomics Solution Sdn Bhd, No. 22A-1, Jalan Bangi Avenue 1/8, Taman Bangi Avenue, 43000 Kajang, Selangor, Malaysia ³Faculty of Applied Sciences, Al-Qalam University Katsina, Katsina, Nigeria ⁴Water Analysis Research Centre, Faculty of Science and Technology, Universiti Kebangsaan Malaysia, 43600 Bangi, Selangor, Malaysia

*Corresponding author: wan.afiq@umt.edu.my

Received: 7 July 2024; Accepted: 25 September 2024; Published: 27 October 2024

Abstract

Amlodipine and nifedipine, both widely used calcium channel blockers (CCBs) for hypertension treatment, have emerged as environmental contaminants in water sources such as lakes, rivers, and oceans due to inadequate effluent treatment. In this study, activated carbon derived from peanut shell waste was utilized in magnetic solid-phase extraction (m-SPE) to determine the presence of amlodipine and nifedipine in water samples. A Plackett-Burman and central composite design were employed to assess the effects of seven parameters: pH, temperature, activated carbon weight, stirring speed, contact time, volume of water sample and desorption solvent. Optimal m-SPE conditions were established as follows: pH 11, water temperature 90°C, stirring speed 500 rpm, contact time 11 minutes, and 1.25 g of activated carbon. High-performance liquid chromatography (HPLC) with a diode array detector was used for the final quantification of the target drugs. The extraction method demonstrated excellent linearity (r² = 0.994) and low limits of detection (LOD) and quantification (LOQ), with LODs of 1.04 ng/mL for amlodipine and 1.13 ng/mL for nifedipine, and LOQs of 3.40 ng/mL for amlodipine and 3.48 ng/mL for nifedipine. Recovery rates ranged from 80% to 98% across three concentration levels. Repeatability analysis indicated satisfactory intra-day and inter-day relative standard deviation below 6%. Regeneration studies on adsorbent performance showed recovery loss rates below 15% after four cycles. Additionally, the m-SPE method was environmentally sustainable, with an overall AGREEnness score of 0.71, Blue Applicability Grade Index (67.5), and Sample Preparation Metric Sustainability (7.47) underscoring its green credentials.

Keywords: greenness profile, magnetic adsorbent, extraction, pharmaceutically active compounds

Abstrak

Amlodipine dan nifedipine, kedua-duanya penghalang saluran kalsium (CCBs) yang digunakan secara meluas untuk rawatan hipertensi, telah muncul sebagai pencemar alam sekitar dalam sumber air seperti tasik, sungai, dan lautan akibat rawatan efluen yang tidak mencukupi. Dalam kajian ini, karbon teraktif yang berasal dari sisa kulit kacang tanah digunakan dalam pengekstrakan fasa pepejal magnetik (m-SPE) untuk menentukan kehadiran amlodipine dan nifedipine dalam sampel air. Rekabentuk Plackett-Burman dan komposit berpusat digunakan untuk menilai kesan tujuh parameter: pH, suhu, berat karbon teraktif, kelajuan pengacauan, masa sentuh, isi padu sampel air dan pelarut nyahjerapan. Keadaan m-SPE yang optimum ditetapkan seperti berikut: pH 11, suhu air 90°C, kelajuan pengacauan 500 rpm, masa sentuh 11 minit, dan 1.25 g karbon teraktif. Kromatografi cecair prestasi tinggi (HPLC) dengan detektor diod tatasusunan digunakan untuk pengkuantitian akhir ubat-ubatan tersebut. Kaedah pengekstrakan menunjukkan kelinearan yang cemerlang (r² = 0.994) dan had pengesanan (LOD) serta had pengkuantitian (LOQ) yang rendah, dengan LOD masing-masing 1.04 ng/mL untuk amlodipine dan 1.13 ng/mL untuk nifedipine, serta LOQ masingmasing 3.40 ng/mL untuk amlodipine dan 3.48 ng/mL untuk nifedipine. Kadar perolehan semula antara 92% hingga 98% di tiga tahap kepekatan. Analisis kebolehulangan menunjukkan sisihan piawai relatif intra-hari dan antara-hari yang memuaskan di bawah 6%. Kajian penggunaan semula terhadap prestasi penjerap menunjukkan kadar kehilangan perolehan semula di bawah 15% selepas empat kitaran. Selain itu, kaedah m-SPE adalah mampan dari segi alam sekitar, dengan skor keseluruhan AGREEnness 0.71, Indeks Gred Ketergunaan Biru (67.5), dan Kelestarian Metrik Penyediaan Sampel (7.47) menekankan kelayakan hijau kaedah ini. Kata kunci: profil kehijauan, penjerap magnetik, pengekstrakan, sebatian farmaseutikal aktif

Introduction

Carbonaceous material derived from natural waste, such as agricultural residues and food scraps, is increasingly being utilized for its environmental and economic benefits. These materials are structurally unique, widely abundant, highly sustainable, and regenerative in nature [1]. The conversion methods involve processes such as pyrolysis, hydrothermal, ionothermal, and gasification, followed by physical or chemical activation, which enhances surface area and porosity. The thermal phase usually involves carbonization in the presence of mild oxidizing gases such as carbon dioxide or steam for surface activation [2]. Physical activation leads to the formation of meso- or micropores, while chemical activation (e.g., using acidic or basic dehydrating agents) helps eliminate undesirable particulates from the surface and relocates functional groups [3]. Chemical activation provides better control over pore structure, enhancing the activated carbon's effectiveness and often resulting in higher yields [4].

The utilization of activated carbon in sample preparation, extraction, or microextraction techniques is highly valued for its effectiveness in capturing and isolating various target analytes. Using this material as a precursor for extraction or removal processes offers several advantages, including cost-effectiveness, sustainability, and high efficiency in adsorbing analytes due to its large surface area, reactivity, chemical resilience, thermal stability, and flexibility in

manipulating its porous structure [5]. Common formulations include powdered activated carbon (PAC), granular activated carbon (GAC), or formed shapes (e.g., extrudates, pellets, tablets), which are chosen based on the specific requirements of the experimental process. Adsorption using activated carbon is a popular method for pollutant removal because of its large surface area. Through mechanism interactions, the pores in activated carbon are larger than the target molecules, allowing these molecules to enter and be adsorbed. Additionally, the attractive forces of activated carbon are stronger than the forces keeping the target analytes dissolved in the solution, leading to effective adsorption on the AC surface and facilitating the mass transfer process [6, 7].

Peanut shells (*Arachis hypogaea*), a form of agricultural waste, have been effectively utilized to extract or remove pollutants from various environments due to their high lignocellulosic content, high polymer materials, and low ash content. This makes them excellent precursors using feasible methods for high-value use [8]. Activated carbon derived from peanut shells exhibits a high surface area and a porous structure, making it highly effective in adsorbing pollutants such as inorganic contaminants (e.g., metals, gases) [9-12] and organic contaminants (e.g., dyes, nitroaromatics, pesticides, pharmaceuticals) [13-17]. Adsorption studies typically show that the kinetics of target analyte removal by peanut shell-based activated carbon follow pseudo-

second-order models, indicating chemisorption. Isotherm models, such as Langmuir and Freundlich, are used to describe the adsorption behaviour, with the Langmuir model often fitting well, suggesting monolayer adsorption on a homogeneous surface. The material can be regenerated and reused multiple times without significant loss of adsorption capacity [18-20].

Magnetically modified activated carbon offers the advantage of easy separation and recovery after catalytic runs or environmental remediation through a simple magnetic process. Literature studies showcase that the fabrication of magnetic peanut shell-derived activated carbon improves analytical performance, including high selectivity, high recovery, high stability, and good regeneration [21, 22]. Existing extraction methods often suffer from inefficiency, time-consuming procedures, and environmental concerns, highlighting the need for more effective and sustainable alternatives. This research aimed to synthesize magnetic peanut shellderived activated carbon and introduce it into the solidphase extraction method for the determination of calcium channel blockers in water samples, making the newly developed method highly efficient, rapid, and environmentally friendly. The synergistic effects influencing the extraction system were investigated through response surface methodology. The analytical performance, including greenness assessment profile, was also studied.

Materials and Methods

Materials and reagents

Amlodipine (C₂₀H₂₅ClN₂O₅ CAS 88150-42-9), and nifedipine (C₁₇H₁₈N₂O₆ CAS 21829-25-4) were purchased from Dr. Ehrenstorfer GmbH (Augsburg, Germany). Standard solutions of the target analytes were prepared in methanol at a concentration of 10 µg/mL. Working standard solutions were prepared by diluting the stock solution with ultrapure water (18.2 M Ω ·cm) obtained from the Milli-O water purification system manufactured by Millipore Corporation (Bedford, MA, USA). All solutions were stored at 4 °C. HPLC-grade methanol, acetonitrile. potassium dihydrogen sodium acetate, sodium hydroxide, phosphate, hydrochloric acid (37%), and nitric acid (65%) were obtained from Merck (Darmstadt, Germany). Iron (II, III) oxide (FeO, Fe₃O₄, respectively) with particle sizes of 50-100 nm was used as a principal constituent to characterize and prepare magnetic peanut shell-derived activated carbon (m-PSAC). This material was purchased from Sigma-Aldrich (Steinheim, Germany).

Preparation of peanut shell-derived activated carbon

Peanut shells were cut into small pieces, washed with distilled water, and subjected to sonication in water for 30 minutes. The supernatant was discarded, and this cycle was repeated three times. The wet shells were then transferred to glass containers and dried in an oven at 80 °C. Once dried, the shells were ground into a fine beige powder using a sample grinder. The powder was sieved to obtain a mesh size range of 300-500 µm and stored in a 150 mL glass container. For the carbonization phase, the powder was placed in a porcelain crucible and heated in a muffle furnace at 500 °C for 20 minutes, with a heating rate of 5 °C/min. The resulting powder was dried in an oven until a constant weight was achieved, then sieved through a 40 µm mesh and stored in a glass vial. The yield of activated carbon was weighed and labelled as peanut shells-derived activated carbon (PSAC). The process was repeated to obtain the desired amount of material for subsequent analyses. A total of 10 g of activated carbon was mixed with 10 g of Fe₃O₄ nanoparticle powder, dissolved in distilled water, and heated at 70 $^{\circ}\text{C}$ for 1 hour. The mixture was then adjusted to pH 10-11 using 1M NaOH and stirred for 1 hour before being cooled to room temperature. The precipitate was rinsed with distilled water and dried at 70 °C overnight in an oven to obtain magnetic peanut shells-derived activated carbon (m-PSAC).

Sorbent characterization and drug analysis

The magnetic properties of m-PSAC were investigated using a Vibrating Sample Magnetometer (VSM; Lakeshore VSM 7404, USA). The magnetic behaviour was recorded at ambient temperature by varying the applied magnetic field from -10 to +10 kG. The surface area and pore size of m-PSAC were determined using a Micromeritics TriStar II system, version 3.0.3 (Micromeritics Instrument Co., Atlanta, Georgia, USA). Measurements were taken at 77.35 K, with the surface area calculated using the Brunauer-Emmett-Teller (BET) method. Pore size distribution and volumes were

assessed using the Barrett-Joyner-Halenda (BJH) method. The FT-IR spectra were obtained using a Fourier Transform Infrared (FT-IR) spectrophotometer (ATR-FTIR; Shimadzu, IRTracer-100, Japan) to examine the functional groups, with a resolution of 4 cm⁻¹ over the range of 4000-400 cm⁻¹. The crystal structure of m-PSAC was analysed by X-ray Diffraction (XRD), with a scanning range of 2θ from 5° to 90° (D8 Quest, Bruker, Germany). The microstructure of the m-PSAC surface was examined using a high-resolution scanning electron microscope (SEM; INSPECT-F50, Thermo Fisher Scientific, FEI, Holland) with images captured at magnifications of 400–5000x.

The detection of target drugs from spiked samples and analytical measurements was conducted using a Shimadzu High-Performance Liquid Chromatography (HPLC) system (Kyoto, Japan). The system was equipped with a solvent delivery module (model LC-40D XS), a degassing unit (model DGU-405), a system controller (model CBM-40), an autosampler (model SIL-40C XS), and a diode-array detector (DAD, model SPD-M40). The stationary phase comprised a ShimPack GIST C18 column (4.6 mm × 150 mm, 5 µm particle size). An isocratic mobile phase of 65% acetonitrile, 15% methanol, and 20% deionized water was used. The column temperature was maintained at 40 °C, with a flow rate of 0.7 mL/min. The Diode Array Detector (DAD) scanned wavelengths from 220 to 280 nm. Amlodipine exhibited maximum absorbance at 233 nm, while nifedipine showed maximum absorbance at 280 nm. Figure 1 presents the chromatogram results for the detection of target drugs in spiked samples, showing varying peak heights due to the differing sensitivity properties of each drug in HPLC detection.

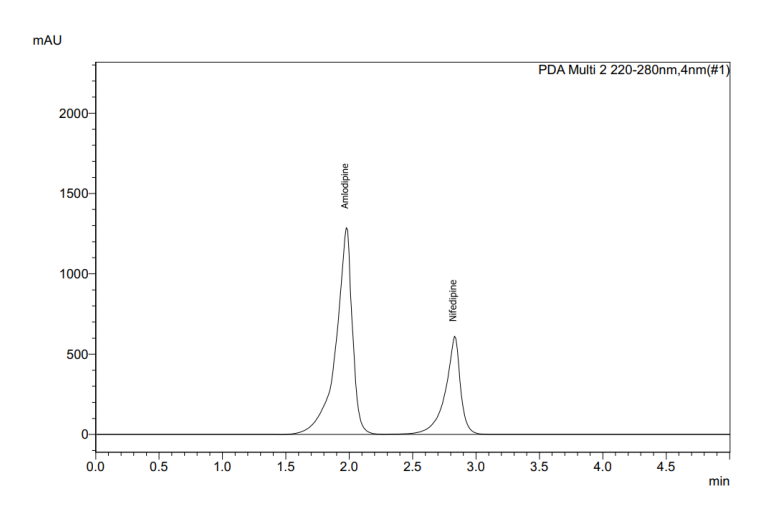


Figure 1. Chromatogram of extracted target analytes in spiked samples

Screening and optimization

The experimental design and statistical analysis were conducted using Statistica Version 14.0.0.15 (TIBCO Software Inc.). In this study, a Plackett–Burman design was utilized to assess the relative significance of various variables affecting the preconcentration of CCB drugs (amlodipine and nifedipine). The Plackett-Burman design efficiently screens multiple variables to identify the most significant factors, while the central composite design refines these key factors to optimize experimental conditions for the best outcomes. The matrix design was constructed from matrices with

orthogonal columns, comprising only (+1) or (-1) levels. The resulting mathematical model is a first-order model that does not include interaction terms. Seven predetermined variables namely volume of water sample (X_1) , pH (X_2) , water temperature (X_3) , weight of m-PSAC (X_4) , stirring speed (X_5) , contact time (X_6) , and volume of desorption solvent (X_7) —were screened across 8 experimental designs (as shown in Table 1). The selection of these variables and their levels was based on their demonstrated influence on extraction efficiency in prior studies and preliminary experiments, as they directly affect adsorption dynamics and analyte

interactions. For the optimization experiments, a central composite design (CCD) model was employed. The variables studied for removal were set at five coded

levels $(-\alpha, -1, 0, +1, +\alpha)$. The amount of drug adsorbed per unit mass of magnetic activated carbon is given by Equation 1.

$$q = \frac{c_o - c_f}{m} \times V \tag{1}$$

Here, q is the amount of CCB drugs adsorbed by the m-PSAC (mg g⁻¹); C_o is the initial concentration in contact with the adsorbent (mg L⁻¹); C_f is the concentration after the experimental study (mg L⁻¹); m is the mass of m-PSAC (g); and V is the volume of the CCB drugs standard solution (L).

The mathematical relationship between the independent variables was modelled by fitting a second-order polynomial equation, allowing the response to be expressed as the quadratic Equation 2 below.

$$Y = \beta_0 + \sum_{i=1}^k \beta_i X_i + \sum_{i=1}^k \beta_i X_i^2 + \sum_{i=1}^k \sum_{i=1}^k \beta_{ii} X_i X_i$$
 (2)

The optimum model encompasses main effects, quadratic effects, and curvature effects, with Y representing the predicted response (removal percentage), and X_i , X_{ij} representing the un-coded parameters. The coefficients of the model, denoted as β_o , β_i , β_{ji} , and β_{jj} , are associated with these effects. It's important to note that the polynomial model serves as a reasonable approximation of the true functional relationship within a limited region of the independent values' space. Desirability functions (DF) were used to optimize the operating parameters in preconcentration process of CCB drugs. To assess the model's adequacy, a comparison between experimental and predicted

responses was conducted using a normal probability plot of the studentized residuals to verify the normality of residuals. Statistical analysis involved assessing the analysis of variance using the Fisher test (*F*-test) alongside the probability test (*P*-value), with a significance level set at 0.05. Validation of the model included comparing calculated values with predicted values and examining the coefficient of determination (R²). Additionally, for visualizing variable interactions and determining optimal process conditions, three-dimensional (3D) plots of the model were utilized for graphical interpretation.

Table 1. The experimental variables and levels of the Plackett-Burman design

Run Order	Volume of Water Sample	pН	Water Temperature	Weight m-PSAC	Stirring Speed	Contact Time	Volume of Methanol
	(mL)		(° C)	(g)	(rpm)	(min)	(μL)
	X ₁	\mathbf{X}_2	X 3	X 4	X 5	X 6	X ₇
3	15	9	45	0.5	400	5	750
4	45	9	45	1	200	5	250
6	45	5	90	0.5	400	5	250
8	45	9	90	1	400	9	750
1	15	5	45	1	400	9	250
2	45	5	45	0.5	200	9	750
5	15	5	90	1	200	5	750
7	15	9	90	0.5	200	9	250

Extraction procedure

Water samples (X_1) were prepared by adding either 15 or 45 mL of deionized water into a 100 mL conical flask. The pH of the water (X_2) was adjusted using 1 N nitric acid or 1 N sodium hydroxide solution, as specified in the run order in Table 1. Afterward, 1 mL of the CCB drug standard solution was added to the water sample and gently stirred with a glass rod to ensure homogeneity. The conical flask was placed on a heater plate, and the water temperature was adjusted to the desired condition (X_3) . A magnetic stirrer bar was then added to the water sample, followed by the specified

amount of m-PSAC (X_4), as indicated in Table 1. The aqueous solution was stirred at a constant speed (X_5). Upon completion of the stirring process (X_6), an external magnet was used to separate the m-PSAC from the solution. The m-PSAC was then transferred into an Eppendorf tube, where the desorption solvent, methanol, was added (X_7), and the mixture was vortexed for 1 minute. The organic layer (methanol) was collected, filtered, and transferred into an HPLC vial for subsequent analysis. The general procedure is illustrated in Figure 2.

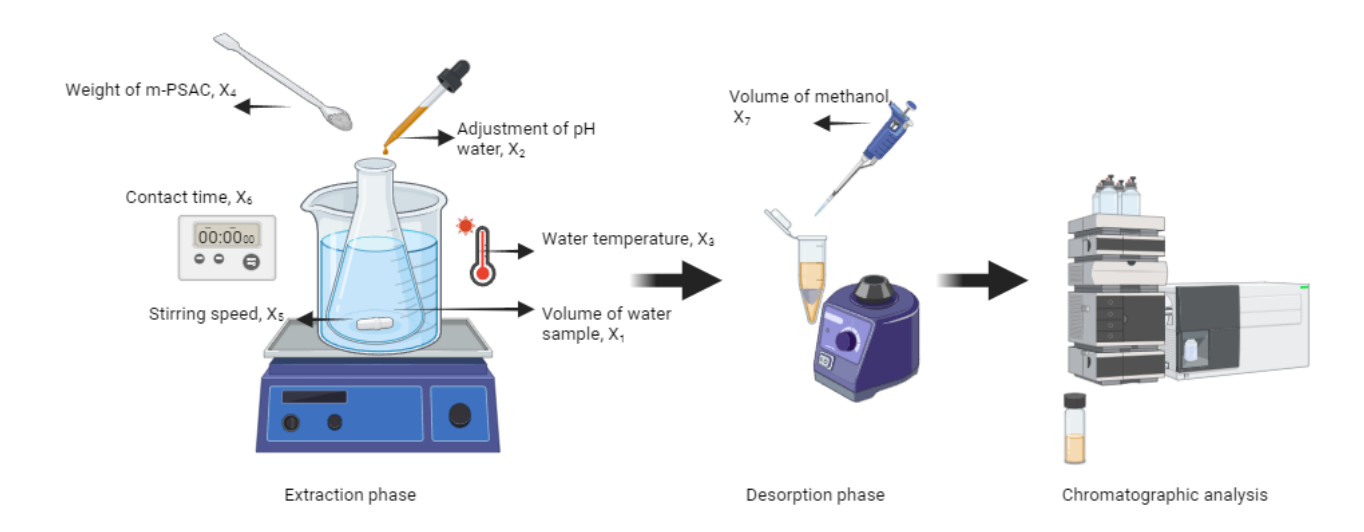


Figure 2. General workflow of magnetic solid phase extraction using m-PSAC

Analytical performance

Linearity test was carried out using standard addition method, concentration level spiked ranging 0.01 to 0.5 ng/mL. To evaluate the accuracy and precision of the method, the extraction condition was applied under repeatable conditions (n = 9) to aqueous sample, which were enriched at the three concentration levels. The accuracy was obtained by calculating the recovery (% recovery), while precision was expressed in terms of the relative standard deviation (RSD). The detection and quantification limits (LOD and LOQ, respectively) of the methodology were calculated as LOD = $3.3~S_{(y/x)}/m$, and the limit of quantification and LOQ = $10~S_{(y/x)}/m$. Here $S_{(y/x)}$ is the standard error of the regression and m is the slope of the calibration curve. Finally, the matrix

effect (ME) was evaluated by comparing the normalized areas of the analytes in a standard prepared in organic solvent and a standard prepared in the presence of the matrix under study. The regeneration of m-PSAC is key criteria for the routine analysis, for this reason, the recovered m-PSAC was washed using methanol and dried to constant weight for use in subsequent regeneration tests, evaluated for 4 cycles.

Greenness profile evaluation

The environmental sustainability of the developed extraction method was assessed using green analytical chemistry metrics. Three key tools—Analytical GREEnness (AGREE), Blue Applicability Grade Index (BAGI), and Sample Preparation Metric Sustainability

(SPMS)—were employed for this evaluation. AGREE, a green analytical chemistry metric, evaluates analytical methods based on the 12 principles of green analytical chemistry. The outcome is depicted as a clock-like pictogram that assesses each principle individually and provides an overall score. This final score, ranging from 0 to 1, indicates how environmentally friendly the method is, with a score closer to 1 denoting greater alignment with green principles [23].

BAGI is a tool used to evaluate the practicality of a method in analytical chemistry, scoring it from 25 to 100, with higher scores indicating greater practicality. Key characteristics assessed include the type of analysis, number of analytes, sample preparation, sample volume, throughput, reagents and materials, instrumentation, and degree of automation, all of which align with the practical aspects of White Analytical Chemistry [24, 25]. BAGI software generates an asteroid pictogram, with individual segments shaded white, light blue, blue, or dark blue to represent no, low, medium, or high compliance with applicability criteria, respectively [26]. The proposed method was evaluated using BAGI 0.9.2 free software and received a BAGI score of 60, demonstrating its applicability.

The SPMS metric assesses 9 parameters divided into 4 categories based on the type of information they provide: (i) sample information (e.g., sample amount, either volume for liquids or weight for solids), (ii) extractant information (e.g., amount, nature, and reusability), (iii) sample preparation procedure information (e.g., number of steps, extraction time, need for additional steps, and sample throughput), and (iv) energy consumption and waste. The score is easily visualized in a clock diagram, where each parameter is represented by a coloured square, except for reusability, which is marked with a star when the extractant can be reused [27].

Results and Discussion

Characterization of m-PSAC

The XRD micrographs presented in Figure 3 show six prominent diffraction peaks. Our study reveals that sharp peaks indicate that the m-PSAC has complete crystallinity, high purity, and that no impurities were introduced during the fabrication process. These sharp peaks correspond to the m-PSAC, appearing at 2θ values of 28.23° (220), 31.57° (311), 45.32° (400), 53.75° (422), 56.33° (511), and 66.28° (400). These peaks are indicative of the insertion of iron ions into the activated carbon. The crystalline phases essentially consist of magnetite, as referenced by the JCPDS No. 75-0033 standard [28, 29]. Additionally, Figure 3(b) reveals lowintensity and broad diffraction peaks in the XRD profile at $2\theta = 22.17^{\circ}$, suggesting the presence of crystalline cellulose on the surface of bare activated carbon. A small peak observed at 43° corresponds to the (100) plane of graphitic carbon. The graphitic carbon phase in the sample contributes to minimal resistance in electrochemical processes due to its good electrical conductivity [30]. The particle size of m-PSAC, calculated using the Debye-Scherrer equation, was found to be 0.62 nm, in contrast to bare PSAC, which recorded a particle size of 3.92 nm.

Figure 4 shows a prominent peak at 544 cm⁻¹, indicative of Fe-O stretching vibrations, confirming the successful incorporation of Fe₃O₄ as a magnetic adsorbent material. Similar Fe-O bond peaks are observed in Figures 4(c) and 4(d) for magnetic activated carbon before and after the extraction processes, respectively, suggesting that the magnetic properties are retained throughout the process. The C=C stretching vibration bond of skeletal aromatic rings appears at 1632 cm⁻¹ [31]. Peaks at 1374 cm⁻¹ and 1037 cm⁻¹ are attributed to C-C and C-N stretching vibrations, respectively. These peaks are found in almost the same wavenumber range in both Figures 4(c) and 4(d), with slight variations in signal intensities before and after extraction, showing increased intensities in the magnetic PSAC [32].

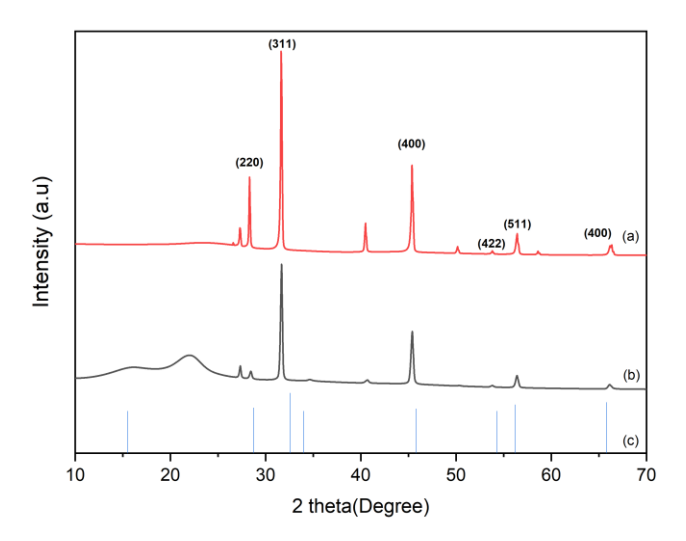
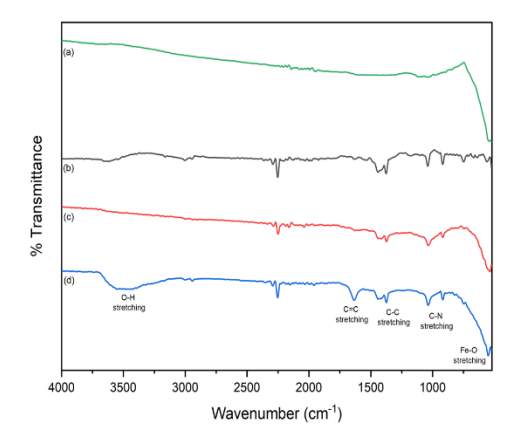


Figure 3. XRD micrographs of (a) bare PSAC, (b) magnetic PSAC and (c) JCPDS No 75-0033

The Vibrating Sample Magnetometer (VSM) analysis, illustrated in Figure 4e, depicts a hysteresis loop resembling the letter 'S', characteristic of typical superparamagnetic behaviour. Saturation magnetization (Ms) is an intrinsic property of magnetic materials, representing the maximum magnetic moment per unit volume for the analysed sample. In this study, the Ms values of m-PSAC were found to be 30.89 emu/g before adsorption (red line) and 27.55 emu/g after adsorption (black line). The Ms value of pure Fe₃O₄ also analysed, calculated at 84 emu/g. The decrease in Ms observed in

this study could be attributed to several factors: the addition of non-magnetic graphene oxide (GO) (referenced as activated carbon) to the synthesized adsorbent, the formation of a magnetic dead layer, inductive effects, or the loss of magnetic nanoparticle aggregates during the desorption phase. Additionally, the coercivity (Hc) and retentivity (Mr) of m-PSAC were calculated to be 152.18 G and 0.621 emu/g, respectively. Coercivity indicates the intensity of the magnetic field required to reduce the material's magnetization to zero after it has been magnetized.



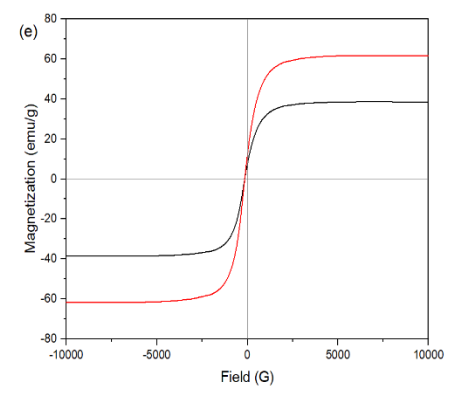


Figure 4. FTIR spectra of (a) Fe₃O₄ nanoparticle, (b) bare PSAC, (c) magnetic activated carbon (pre-extraction), (d) magnetic activated carbon (post extraction), and (e) VSM graph for m-PSAC

Figure 5(a) illustrates the surface of bare activated carbon, which exhibits an irregular and rough texture. The SEM micrographs reveal an absence of pores on the external surface. This observation aligns with findings from [33], use SEM to study activated carbon derived from peanut shells for CO₂ absorption. Initially, the surface of the activated carbon lacked pores, but after chemical activation, numerous interconnected pore structures developed, significantly enhancing CO₂ adsorption capacity. The Energy Dispersive X-ray

(EDX) analysis results for bare activated carbon are shown in Figure 5(c). The EDX spectrum indicates a high carbon content (98.22%), which is typical for carbonaceous materials, along with a trace presence of iron (1.78%), likely originating from the natural composition of peanut shells. The surface morphology of both bare and magnetic activated carbon was characterized using SEM-EDX analysis, as shown in Figures 5(a) and 5(b).

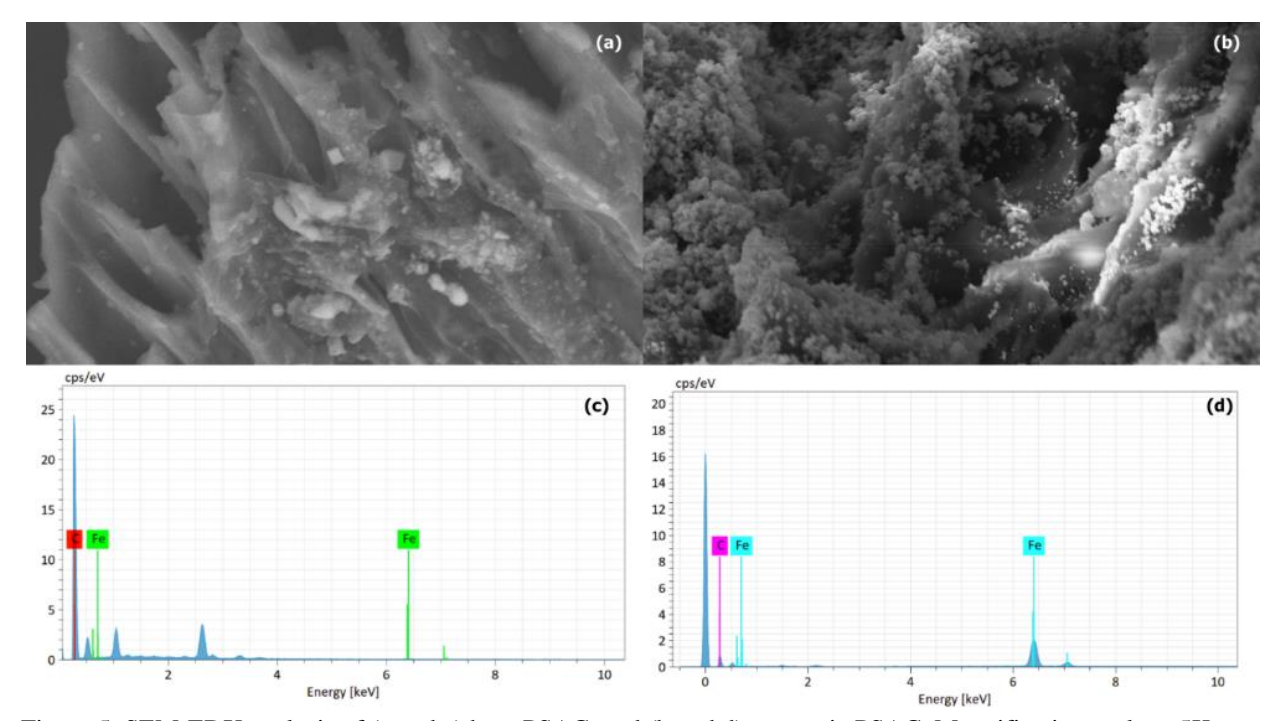


Figure 5. SEM-EDX analysis of (a and c) bare PSAC, and (b and d) magnetic PSAC. Magnification scale at 5Kx

Figure 5(b) presents SEM micrographs of magnetic activated carbon after treatment with NaOH. The surface shows numerous white cavities and an uneven distribution of Fe₃O₄ nanoparticles, likely due to NaOH-induced degradation. Nascimento et al. [34] characterized magnetic activated carbon and noted that surface cavities enhance adsorption effectiveness. These cavities allow analyte dye molecules, such as brilliant blue dyes, to pass through the adsorbent and enter the pores, thereby improving removal from environmental water. The EDX spectrum for magnetic PSAC is shown in Figure 5(d). The composition analysis reveals a significant difference in the percentages of carbon and iron elements compared to bare activated carbon.

Magnetic PSAC contains 18.48% carbon and 81.52% iron, indicating a substantial increase in iron content after the addition of Fe₃O₄.

Both the adsorption isotherm curve and the particle size distribution plot (Figure 6) exhibit a type IV isotherm with a type H4 hysteresis loop, according to the IUPAC classification. The increase in N_2 uptake during the adsorption phase at higher relative pressure (above $p/p^\circ = 0.6$) suggests that the Fe₃O₄ cavities on the activated carbon are layered, indicating the material's mesoporous structure. The fabrication of magnetic particles on activated carbon noticeably enhances the adsorption capacities of m-PSAC, providing additional sorption

sites for magnetic carbonaceous composites, as observed in several earlier studies. The average pore size is concentrated in the mesoporous range (2-50 nm) for m-PSAC. Activated carbon with a high surface area and

mesoporous structure is effective for the adsorption of macromolecules like CCB drugs, as these bulky molecules can easily diffuse into the mesopores and adsorb onto the surface of the activated carbon pores.

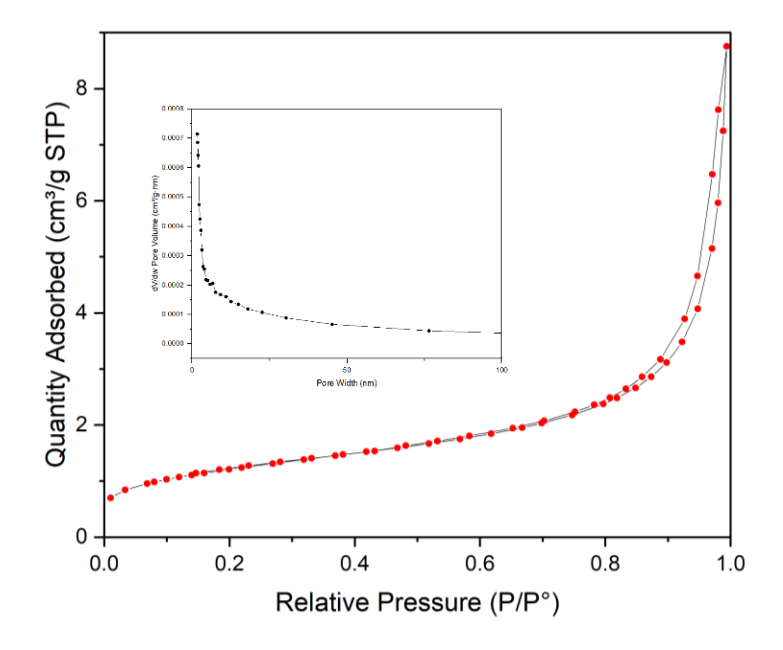


Figure 6. N₂ adsorption-desorption isotherm at 77.3 K and (insert) pore size distribution of m-PSAC

Screening and optimization of magnetic solid phase extraction method

Based on the Pareto chart (Figure 7), the weight of m-PSAC (X_4) exhibits the greatest influence on the extraction system. In contrast, the volume of methanol (X_7) and the volume of the water sample are not significant variables, as their bars do not cross the red reference line on the Pareto chart, indicating insignificance at the 95% confidence level. Consequently, these variables were held constant

throughout the optimization procedure. The five significant variables namely weight of m-PSAC (X_4), contact time (X_6), stirring time (X_5), water temperature (X_3), and pH (X_2) were selected for optimization using a central composite design, which included a total of 27 experimental run orders. Table 2 displays the central composite design, detailing all the variables investigated in this study. The developed mathematical model, based on the quadratic regression equation, is presented as follows:

$$\begin{aligned} \text{Total Peak Areas} &= 6990484 - 749082X_2 + 27073X_2^2 - 11835X_3 + 58X_3^2 - 13847X_4 + 5X_4^2 - 402931X_5 + 7258X_5^2 \\ &- 1799238X_6 + 6011950X_6^2 + 283X_1X_2 + 243X_1X_3 + 17745X_1X_4 + 106853X_1X_5 + 9X_2X_3 + 508X_2X_4 - 3372X_2X_5 + 1952X_3X_5 - 1936X_4X_5 \end{aligned}$$

A variable with a high positive coefficient indicates a strong positive effect on the response, while a negative coefficient demonstrates an inverse relationship, meaning that decreasing the variable will enhance the response. Analysis of variance (ANOVA) at a 95% confidence level was used to assess the statistical

significance of the experimental design, with the results presented in Table 3. A model with a large F-value and a small p-value (<0.05) is considered statistically significant. The R^2 and adjusted R^2 values were observed to be 0.98 and 0.95, respectively. These high values indicate that the model explains more than 98%

of the variability in the experimental data, suggesting that less than 2% of the total variations in both contaminants cannot be described by the model. Additionally, the predicted R² value of 0.93 reflects the model's ability to predict new responses, and it is in close agreement with the R² value. Another measure of the model's statistical significance is the precision value,

which represents the signal-to-noise ratio. In this study, the adequate precision was 18.85. Models with an adequate precision greater than 4 are considered reliable in the context of central composite design (CCD). The coefficient of variation (C.V. %) of the model is 7.63, which is very low and indicates the model's reliability and repeatability.

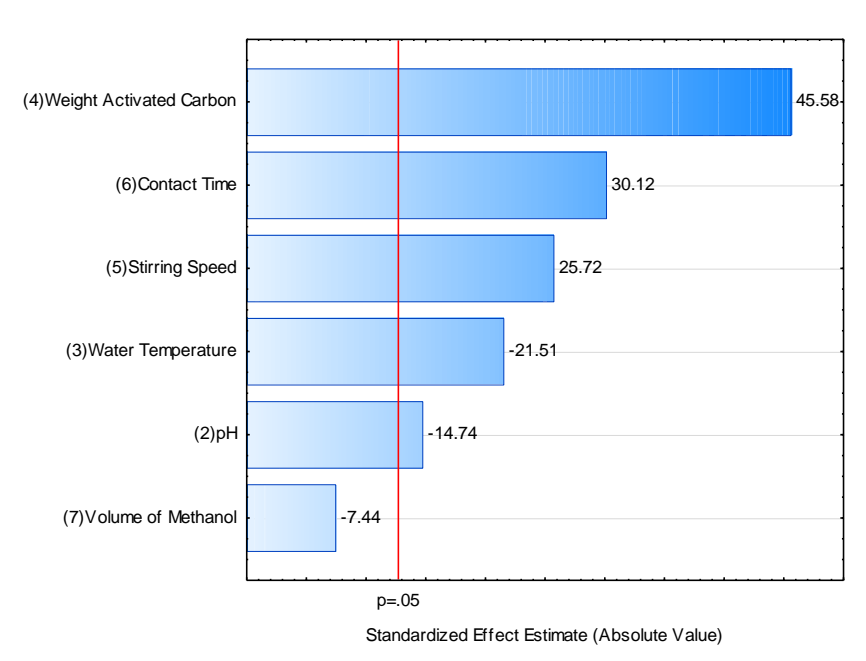


Figure 7. Pareto chart for the variables studied using Plackett-Burman design

Table 2. Experimental design matrix and response (chromatographic and adsorbent capacity)

	F -		· -		~··		· · · · · · · · · · · · · · · · · · ·
Run Order	pН	Water	Weight	Stirring	Contact	Total	Adsorption
		Temperature	m-PSAC	Speed	Time	Peak Areas	Capacity
	X_2	X 3	X 4	X 5	X ₆		$(mg g^{-1})$
1	9	90	0.5	200	9	3105228	0.043
2	5	90	1	400	5	3870367	0.054
3	7	68	1.25	300	7	2707502	0.038
4	5	90	1	200	9	3473069	0.048
5	9	90	1	200	5	6913313	0.096
6	7	113	0.75	300	7	1577472	0.022
7	5	45	0.5	400	5	3373084	0.047
8	9	45	0.5	200	5	6686628	0.093
9	3	68	0.75	300	7	915368	0.013
10	9	90	0.5	400	5	4901894	0.068
11	9	45	1	400	5	12914149	0.180
12	11	68	0.75	300	7	9153685	0.128
13	7	68	0.75	300	7	2707502	0.038
14	7	68	0.75	300	11	1469913	0.020

Sukardan et al.: HARNESSING OF PEANUT SHELL WASTE-DERIVED ACTIVATED CARBON FOR EFFICIENT MAGNETIC SOLID PHASE EXTRACTION OF CALCIUM CHANNEL BLOCKERS DRUGS FROM WATER

15	5	45	1	200	5	7058483	0.098
16	9	45	0.5	400	9	10667579	0.149
17	5	90	0.5	400	9	4767679	0.066
18	9	45	1	200	9	11208289	0.156
19	7	68	0.75	500	7	343510	0.005
20	7	23	0.75	300	7	157747	0.002
21	5	45	0.5	200	9	5338046	0.074
22	5	45	1	400	9	5081927	0.071
23	7	68	0.75	100	7	2231967	0.031
24	5	90	0.5	200	5	5939334	0.083
25	7	68	0.75	300	3	146991	0.002
26	7	68	0.25	300	7	270750	0.004
27	9	90	1	400	9	2627637	0.037

Table 3. ANOVA for analysis of variance and adequacy of the quadratic model

Variable	Sum of Squares ^a	df	Mean Square ^a	F-value	p-value
pH (L)	5569	1	5569	12.117	0.013s
pH (Q)	1876	1	1876	40.825	0.008
Water Temperature(L)	330.8	1	330.8	7.194	0.042^{s}
Water Temperature(Q)	136.8	1	136.8	2.977	0.060
Stirring Speed(L)	330.6	1	330.6	7.194	0.042^{s}
Stirring Speed(Q)	403.2	1	403.2	8.772	0.038^{s}
Contact Time(L)	48.8	1	48.8	1.063	0.075
Contact Time(Q)	134.8	1	134.8	2.934	0.060
Weight m-PSAC (L)	577.4	1	577.4	12.563	$0.030^{\rm s}$
Weight m-PSAC (Q)	226.4	1	226.4	4.927	0.050
X_2 by X_3	25.9	1	25.9	0.564	0.082
X_2 by X_5	3529	1	3529	7.678	0.032^{s}
X_2 by X_6	806.0	1	806.0	17.537	0.023^{s}
X_2 by X_4	456.7	1	456.7	9.936	0.035^{s}
X_3 by X_5	64.4	1	64.4	0.140	0.072
X_3 by X_6	83.7	1	83.7	1.822	0.068
X_3 by X_4	57.5	1	57.5	1.252	0.073
X_5 by X_6	1336	1	1336	29.081	0.013^{s}
X_5 by X_4	381.2	1	381.2	8.293	0.039^{s}
X_6 by X_4	1.4	1	1.4	0.003	0.098
Pure Error	27.57	6	459.6		
Total SS	18460	26			

 $^{^{\}rm a}$ actual value multiply $10^{\rm 6}$, s mean statistically significant at p <0.05

The optimal experimental work was obtained using preparation condition as: 1.25 g weight of m-PSAC (X_4) , 11 min of contact time (X_6) , speed controlled at 500 stirring time (X_5) , adjustment of water temperature

at 80-113 °C (X₃), and pH 11 (X₂), as illustrated in Figure 8. Through additional quadruplicate experiments, it was observed that the experimental values obtained were in good agreement with the values

suggested from the models, with relatively small errors exhibit between the predicted and the actual values, RSD <5%. A desirability value of 0.98 indicated that the estimated function showed good agreement with the

experimental model and desired conditions. The range of desirability is always between 0 and 1 (lowest desirability to highest desirability).

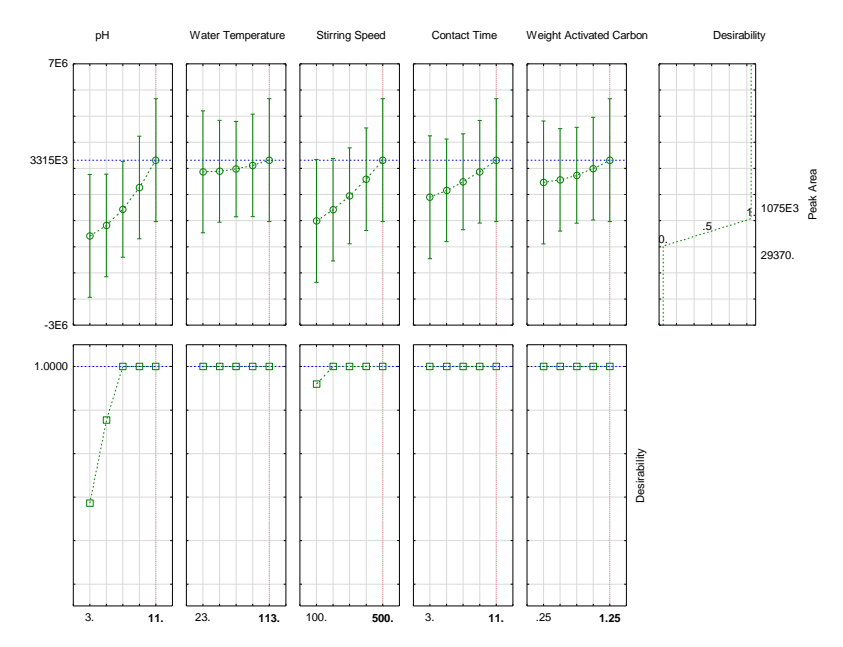


Figure 8. Optimizer plots for studied variables

Figure 9 illustrates the consistency of variance error, represented by the residuals versus the expected normal value dataset. The residuals' normal plot suggests that the data are normally distributed, in good agreement, and utilized to verify normality. Additionally, the data's proximity to the straight line indicates a normal distribution for errors with a constant variance and zero mean [35]. The closer the data points are to the straight line, the higher the correlation and reliability between the predicted and observed values, resulting minimal deviation. Additionally, the residuals were scattered randomly around ± 3.00 , demonstrating that the residual distribution of the regression equation follows normal and independent patterns. This reveals an excellent relationship with high adequacy between experimental and predicted values of the response.

3D response surface

The pH of the water can significantly influence the extraction of amlodipine and nifedipine by altering the ionization states of the drugs and the surface properties

of the magnetic activated carbon (m-PSAC). For instance, amlodipine has a basic amine group that can be protonated or deprotonated. In a basic solution, the amine group is typically deprotonated, making the molecule more neutral. This increases hydrophobic interactions between the drug molecules and the activated carbon, thereby enhancing adsorption. Additionally, a basic pH tends to make the surface of the activated carbon more negatively charged due to the deprotonation of surface functional groups [36]. The relationship between pH (X2) and the weight of m-PSAC (X₄) was further explored using 3D response surfaces, as shown in Figure 10a. A strong positive interaction between these two variables was observed. The red zone on the 3D response curve indicates the ideal conditions where both variables are optimized. This interaction contributes 13.02% to the efficiency of the extraction phase. Adjusting the pH of the water before the adsorption process can also significantly reduce the required contact time, with a 22.98% contribution to extraction efficiency.

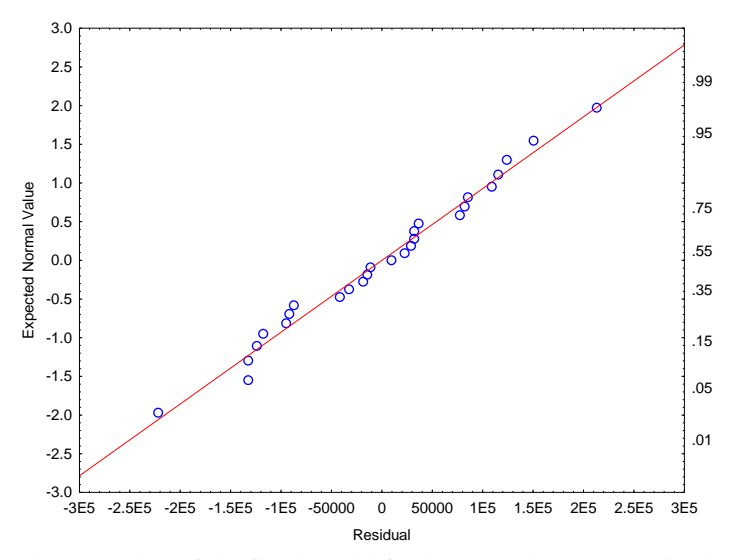


Figure 9. The adequacy plots of the fitted model for the CCB drugs adsorption by the m-PSAC

Water temperature plays a crucial role in the extraction of amlodipine and nifedipine using m-PSAC. Higher temperatures generally enhance solubility, diffusion, and adsorption kinetics but can also increase desorption rates. Elevated temperatures increase the kinetic energy of the drug molecules, leading to faster adsorption rates as the molecules collide more frequently and energetically with the activated carbon surface [37]. This relationship is illustrated in Figure 10b, where the optimal region shows a constant ridge response surface with elongated ellipses. Higher temperatures can improve hydrophobic interactions, which are essential for the adsorption of non-polar or slightly polar molecules like amlodipine and nifedipine.

The stirring rate significantly affects the kinetics of the extraction process. Proper stirring enhances mass transfer, ensures homogeneous distribution, prevents aggregation, and improves adsorption kinetics. A higher stirring rate facilitates the mass transfer of CCB drugs from the bulk solution to the m-PSAC surface by reducing the boundary layer thickness around the

adsorbent particles, thus promoting faster diffusion. Efficient stirring rates prevent aggregation of magnetic activated carbon particles, which can decrease the effective surface area available for adsorption and reduce overall efficiency [38, 39]. This relationship contributes up to 38.11% to extraction efficiency, as shown in Figure 10c.

Adequate contact time is essential to ensure that the adsorption process reaches equilibrium, maximizing the use of the adsorbent's capacity. However, excessively long contact times may lead to desorption and reduced efficiency. Initially, adsorption occurs rapidly due to the abundance of available active sites on the m-PSAC surface, driven by surface diffusion. As time progresses (6-11 minutes), the rate of adsorption slows as the active sites become occupied, transitioning to pore diffusion where molecules diffuse into the internal pores of the activated carbon [40]. The relationship between contact time and weight of m-PSAC on extraction efficiency is illustrated in Figure 10d.

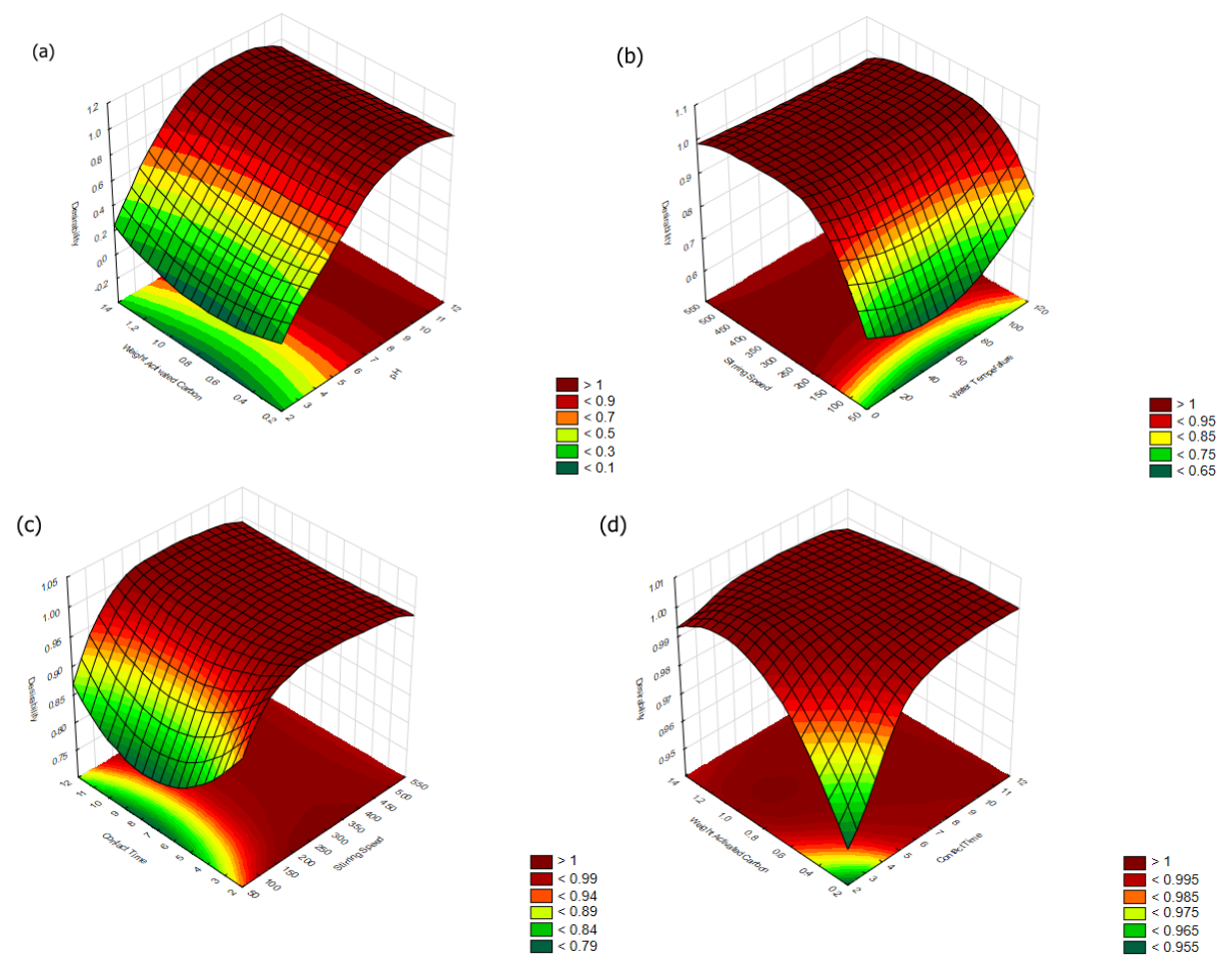


Figure 10. (a) 3D response of interaction term between pH vs weight of m-PSAC, (b) water temperature vs string speed, (c) string speed vs contact time, and (d) contact time vs weight of m-PSAC

Mechanism of interaction

The mass transfer of target analytes into m-PSAC involves several mechanisms: Van der Waals forces, electrostatic interactions, π - π interactions, hydrophobic interactions, and pore filling (Figure 11). Hydrophobic interactions are particularly significant, as both drugs are relatively hydrophobic, making them attracted to the non-polar surface of the activated carbon. CCB drugs readily adhere to the hydrophobic surface of m-PSAC due to their solubility characteristics—0.0074 g/L for amlodipine and 0.0003 g/L for nifedipine [41]. π - π interactions also play a role, as the aromatic rings in the

drugs interact with the aromatic structures in the activated carbon through π - π stacking. The presence of activated carbon strengthens these π - π interactions due to the numerous active centres in the pharmaceutical drugs [42]. Additionally, the –NH groups in the CCB drugs can act as strong electron donors, enhancing the electron density of the aromatic rings. Resonance-induced shifts can cause the nitrogen in the CCB drugs to transition from a proton acceptor to a proton donor [43], further facilitating interaction with the activated carbon.

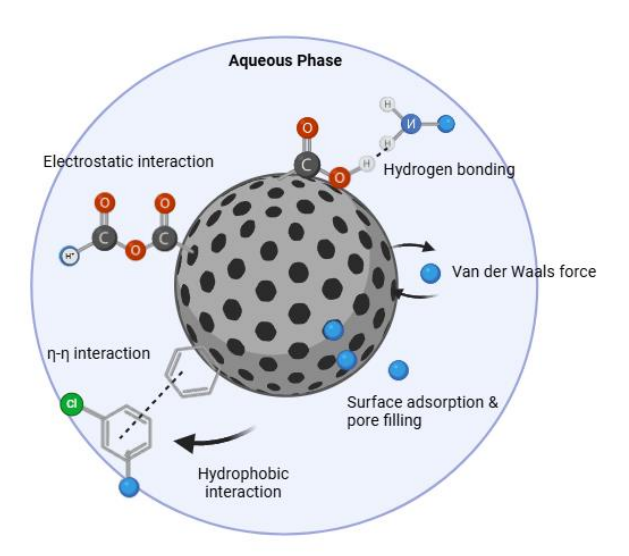


Figure 11. Main mechanism of interaction between m-SPE and target analytes

Analytical performance

Both amlodipine and nifedipine demonstrated good linearity, with determination coefficient values (r²) of 0.994 and 0.990, respectively (Table 4). Higher r² values indicate a better fit of the data to the regression line, suggesting enhanced precision and accuracy in the analytical process. Achieving r² values close to 1 is particularly desirable for concentrations below 1 ppm (or ppb level), as it signifies a strong linear relationship between concentration and the reaction signal, enabling precise monitoring of low concentrations. The limits of detection (LOD) and limits of quantification (LOQ) for amlodipine were 1.04 ng/mL and 3.40 ng/mL,

respectively, while for nifedipine, the LOD and LOQ were 1.13 ng/mL and 3.48 ng/mL, respectively. The low LOD and quantification LOQ achieved during optimization indicate the method's high sensitivity, allowing for the accurate detection and measurement of even trace amounts of analytes. Comparatively, Rajendran et al. [44] reported an LOD of 1.3 ng/mL for nifedipine, while Vidyadhara et al. [45] reported LOD and LOQ values of 0.33 ng/mL and 1.01 ng/mL, respectively, for nifedipine. Our study demonstrated superior sensitivity, detecting nifedipine at significantly lower concentrations than these reported values.

Table 4. Performance characteristics of the proposed method using m-PSAC

Assay		Amlodipine	Nifedipine
Linearity range (ng/mL)		10-500	10-500
Coefficient of determination (r ²)		0.994	0.990
Regression equation		$y = 9x10^6x + 4x10^6$	$y = 8x10^6x + 4x10^6$
Extraction recovery (%)	Deionised Water	94.10-98.72	92.42-98.92
	Wastewater	80.37-82.72	80.84-91.62
	Tap Water	85.06-89.23	85.50-89.88
Matrix Effect (%)		3.71	7.22
Repeatability (%RSD)	Intra-Day	3.65-8.38	1.9-10.11
	Inter-Day	2.46-9.07	2.92-10.7
Limit of detection (ng/mL)	$3.3 S_{(y/x)}/m$	1.04	1.13
Limit of quantification (ng/mL)	$10 \mathrm{S}_{(y/x)} / \mathrm{m}$	3.40	3.48
Regeneration (% Recovery loss)		13.34	12.33

The proposed method also achieved high recovery rates (>90%), indicating effective migration of CCB drugs from the aqueous solution to the m-PSAC surface. The accuracy of the method, ranging from 70% to 120%, falls within the acceptable range for concentration spikes in parts per billion (ppb). Generally, a recovery percentage close to 100% is preferred for concentrations below 1 ppm (or ppb), as it signifies minimal bias and reliable measurement of low concentrations. In contrast, Heidari et al. [46] reported less than 75% extraction recovery for amlodipine using carbon-coated Fe₃O₄ as an adsorbent, highlighting the superior efficacy of our method.

Our method's precision is further demonstrated by the calculated relative standard deviation (RSD) values, which remained below 10% for both amlodipine and nifedipine. These low RSD values indicate high precision, with experimental data tightly clustered around the mean. Typically, lower RSD values are expected at higher concentrations due to stronger signals reducing relative variance. Our method achieved an impressive %RSD of less than 10%, compared to Tamilselvam et al.'s [41] method, which had an %RSD of less than 11% for amlodipine extraction (Table 5). This improvement underscores the enhanced precision and repeatability of our methodology. Additionally, low signal-to-noise ratios can contribute to higher relative variance and %RSD values, further emphasizing the significance of our study's achievement in attaining such low %RSD values.

Greenness profile evaluation

This study highlights significant advancements in environmental sustainability, as evidenced by the AGREE metric program. As illustrated in Figure 12a, the overall score achieved an outstanding 1.0, indicating a high level of "greenness" in the developed method. The extraction technique received a total score of 0.71, reflecting its suitability as a green analytical approach

for analysing pharmaceutical drugs. Despite the use of HPLC, which is not traditionally considered green, its inclusion did not detract significantly from the overall green score, given its optimal performance for the extraction procedure. The AGREE metric evaluated several factors, including sample treatment, device positioning, sample preparation steps, absence of derivatization, and low toxicity, confirming that the method adhered to green analytical chemistry standards. In comparison, Tamilselvam et al. [44] reported a green metric value of 0.68 using a deep eutectic solvent, demonstrating that our method represents a notable improvement in green practices. Future enhancements could include reducing the water sample volume to below 10 mL for smaller-scale applications and utilizing syringe-type dispensers for narrower surfaces. These adjustments could further optimize the method for specific applications and reinforce our commitment to green practices.

The BAGI pictogram for the proposed method, shown in Figure 12b, achieved a score of 67.5, indicating good method applicability. This score reflects high sample throughput, simple instrumentation (HPLC-DAD), straightforward material fabrication, and good sensitivity that negates the need for complex preconcentration. Future improvements could involve analysing multiple analytes (within similar or different therapeutic classes) simultaneously and reducing the sample volume to below 10 mL to enhance the BAGI score. The SPMS score of 7.47 highlights the method's miniaturized procedures, use of natural-based extractants, and low waste production. Improvements in greenness include the use of carbon-based materials and reusability of extractants, contributing to highthroughput capabilities. Future work should focus on energy consumption to address any remaining shortcomings. Techniques such as energy-free dispersion methods could enhance the sustainability and overall greenness of the analytical process.

Table 5. Analytical performance data obtained by using different extraction method in determination of target analytes

Method	Sample	Extraction Solvent/Sorbent	Linearity Coefficient	ER (%)	Detection Limit (µg/L)	RSD (%)	Instrument	Ref.
SPE	Water	HLB	0.995	78 (NIF)	0.0059 (NIF)	<5.2	LC-TOF-MS	[47]
SPE	Water	MCX	0.997	102 (AML)	0.001 (AML)	15	LC-MS/MS	[48]
QuEChERS	Plasma	Acetonitrile	>0.999	96 (AML) and 97 (NIF)	0.014 (AML) and 0.012 (NIF)	<10	UPLC-MS/MS	[49]
MET-DLLME	Water	[BMiM][PF ₆]	0.992	78 (NIF)	1.3 (NIF)	3.32	HPLC-DAD	[44]
USAEME	Plasma	1-Octanol	>0.999	82.6 (AML) and 66.7 (NIF)	0.17 (AML) and 0.15 (NIF)	<5.2	HPLC-UV	[50]
EP-DLLME	Water	Thymol: Decanoic Acid	0.996	96 (AML) and 98 (NIF)	1.73 (AML) and 0.37 (NIF)	<11	HPLC-DAD	[41]
Magnetic SPE	Plasma	Carbon-coated Fe ₃ O ₄	0.999	60 (AML)	0.28 (AML)	<6	HPLC-UV	[46]
Magnetic SPE	Water	Activated Carbon	0.990-0.994	99 (AML) and 98 (NIF)	1.04 (AML) and 1.13 (NIF)	<10	HPLC-DAD	This Study

AML: Amlodipine; NIF: Nifedipine; DLLME: Dispersive Liquid-Liquid Microextraction; EP: Effervescence Powder; HLB: Hydrophilic Lipophilic Balance; IL: Ionic Liquid; MCX: Mixed Cation Exchange; MET: Magnetic Effervescence Tablet; USAEME: Ultrasound-Assisted Emulsification Microextraction; QuEChERS: Quick, Easy, Cheap, Effective, Rugged and Safe

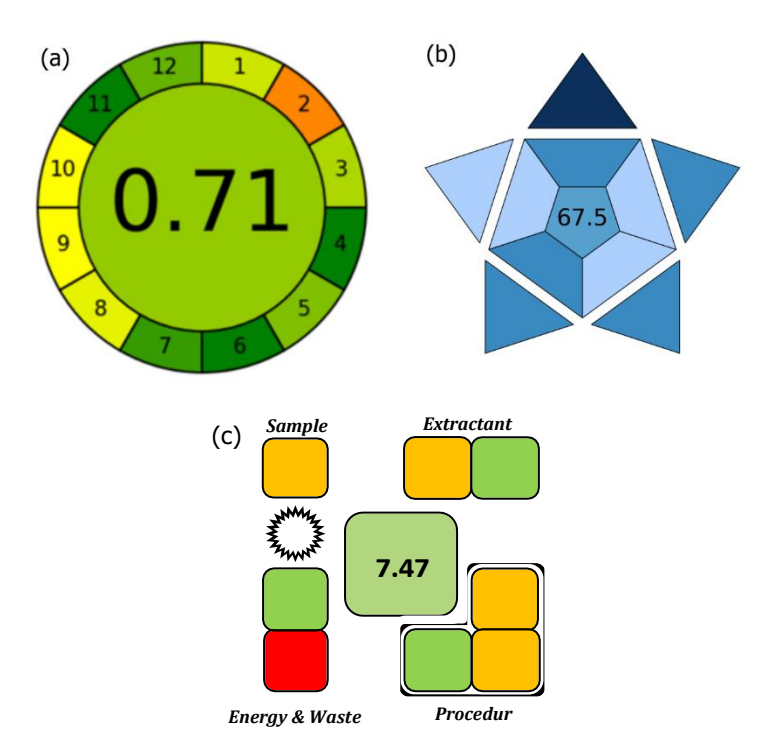


Figure 12. Greenness evaluation score of developed method using (a) AGREE and (b) BAGI and (c) SPMS metric tools

Conclusion

The magnetic solid-phase extraction (m-SPE) method developed in this study presents a practical, straightforward, and environmentally friendly solution for extracting target drugs from water samples. By using activated carbon derived from peanut shell waste and magnetizing it with iron oxide, the method leverages the magnetic properties of the sorbent for easy retrieval and reuse, significantly enhancing the efficiency of drug adsorption. This method is not only rapid, completing the extraction process in just 11 minutes, but also userfriendly. It demonstrates high performance with a broad linear range (10-500 ng/mL), excellent sensitivity, and good recovery rates (>80%). Additionally, it shows low relative standard deviation (RSD) values (<10%) and acceptable limits of detection (LOD) and quantification (LOQ). The sorbent's effectiveness is maintained for up to four cycles, highlighting its durability and costeffectiveness. In terms of environmental sustainability, the m-SPE method excels with an overall AGREE score of 0.71, indicating strong green credentials. The Blue Applicability Grade Index of 6.75 and the Sample Preparation Metric Sustainability score of 7.47 further demonstrate the method's good applicability and low environmental impact. The use of carbon-based materials, such as activated carbon, plays a crucial role in meeting green criteria by improving efficiency, reducing waste, and enabling resource reuse, thus minimizing the environmental footprint of the extraction process.

Acknowledgements

The authors would like to thank Universiti Malaysia Terengganu for its financial support for the study under the analytical and environmental chemistry programme.

References

- 1. Benny, L., John, A., Varghese, A., Hegde, G., and George, L. (2021). Waste elimination to porous carbonaceous materials for the application of electrochemical sensors: recent developments. *Journal of Cleaner Production*, 290: 125759.
- Girgis, B. S., Yunis, S. S., and Soliman, A. M. (2002). Characteristics of activated carbon from peanut hulls in relation to conditions of preparation. *Materials Letters*, 57(1): 164-172.
- 3. Durga, M. L., Gangil, S., and Bhargav, V. K. (2022). Conversion of agricultural waste to

- valuable carbonaceous material: brief review. *Materials Today: Proceedings*, 56: 1290-1297.
- Saravanan, K. A., Prabu, N., Sasidharan, M., and Maduraiveeran, G. (2019). Nitrogen-self doped activated carbon nanosheets derived from peanut shells for enhanced hydrogen evolution reaction. *Applied Surface Science*, 489: 725-733.
- Zhang, S., Tao, L., Jiang, M., Gou, G., and Zhou, Z. (2015). Single-step synthesis of magnetic activated carbon from peanut shell. *Materials Letters*, 157: 281-284.
- Garg, D., Kumar, S., Sharma, K., and Majumder, C.
 B. (2019). Application of waste peanut shells to form activated carbon and its utilization for the removal of Acid Yellow 36 from wastewater. Groundwater for Sustainable Development, 8: 512-519.
- Gayathiri, M., Pulingam, T., Lee, K. T., and Sudesh, K. (2022). Activated carbon from biomass waste precursors: Factors affecting production and adsorption mechanism. *Chemosphere*, 294: 133764.
- 8. Wang, S., Nam, H., and Nam, H. (2020). Preparation of activated carbon from peanut shell with KOH activation and its application for H₂S adsorption in confined space. *Journal of Environmental Chemical Engineering*, 8(2): 103683.
- Zhang, J., Wang, R., Cao, X., Li, Y., and Lan, Y. (2014). Preparation and characterization of activated carbons from peanut shell and rice bran and a comparative study for Cr (VI) removal from aqueous solution. *Water, Air, & Soil Pollution*, 225: 1-10.
- Wilson, K., Yang, H., Seo, C. W., and Marshall, W. E. (2006). Select metal adsorption by activated carbon made from peanut shells. *Bioresource Technology*, 97(18): 2266-2270.
- 11. Al-Othman, Z. A., Ali, R., and Naushad, M. (2012). Hexavalent chromium removal from aqueous medium by activated carbon prepared from peanut shell: adsorption kinetics, equilibrium and thermodynamic studies. *Chemical Engineering Journal*, 184: 238-247.
- 12. Yaman, M., and Demirel, M. H. (2021). Synthesis and characterization of activated carbon from

- biowaste-peanut shell and application to preconcentration/removal of uranium. *Bulletin of Environmental Contamination and Toxicology*, 106: 385-392.
- Georgin, J., Dotto, G. L., Mazutti, M. A., and Foletto, E. L. (2016). Preparation of activated carbon from peanut shell by conventional pyrolysis and microwave irradiation-pyrolysis to remove organic dyes from aqueous solutions. *Journal of Environmental Chemical Engineering*, 4(1): 266-275.
- 14. Ahmad, M. A., Yusop, M. F. M., Zakaria, R., Karim, J., Yahaya, N. K. E., Yusoff, M. A. M., ... and Abdullah, N. S. (2021). Adsorption of methylene blue from aqueous solution by peanut shell based activated carbon. *Materials Today: Proceedings*, 47: 1246-1251.
- 15. Tomul, F., Arslan, Y., Kabak, B., Trak, D., Kendüzler, E., Lima, E. C., and Tran, H. N. (2020). Peanut shells-derived biochars prepared from different carbonization processes: comparison of characterization and mechanism of naproxen adsorption in water. Science of the Total Environment, 726: 137828.
- Orduz, A. E., Acebal, C., and Zanini, G. (2021).
 Activated carbon from peanut shells: 2, 4-D desorption kinetics study for application as a green material for analytical purposes. *Journal of Environmental Chemical Engineering*, 9(1): 104601.
- 17. Xu, W., Zhao, Q., Wang, R., Jiang, Z., Zhang, Z., Gao, X., and Ye, Z. (2017). Optimization of organic pollutants removal from soil eluent by activated carbon derived from peanut shells using response surface methodology. *Vacuum*, 141: 307-315.
- Gonzo, E. E., and Gonzo, L. F. (2005). Kinetics of phenol removal from aqueous solution by adsorption onto peanut shell acid-activated carbon. *Adsorption Science & Technology*, 23(4): 289-302.
- 19. Zhang, J. X., and Ou, L. L. (2013). Kinetic, isotherm and thermodynamic studies of the adsorption of crystal violet by activated carbon from peanut shells. *Water Science and Technology*, 67(4): 737-744.
- 20. Tanyildizi, M. Ş. (2011). Modeling of adsorption isotherms and kinetics of reactive dye from aqueous

- solution by peanut hull. *Chemical Engineering Journal*, 168(3): 1234-1240.
- 21. Aryee, A. A., Mpatani, F. M., Dovi, E., Li, Q., Wang, J., Han, R., ... and Qu, L. (2021). A novel antibacterial biocomposite based on magnetic peanut husk for the removal of trimethoprim in solution: Adsorption and mechanism study. *Journal of Cleaner Production*, 329: 129722.
- 22. Aryee, A. A., Mpatani, F. M., Zhang, X., Kani, A. N., Dovi, E., Han, R., ... and Qu, L. (2020). Iron (III) and iminodiacetic acid functionalized magnetic peanut husk for the removal of phosphate from solution: characterization, kinetic and equilibrium studies. *Journal of Cleaner Production*, 268: 122191.
- Pena-Pereira, F., Wojnowski, W., and Tobiszewski, M. (2020). AGREE—Analytical GREEnness metric approach and software. *Analytical Chemistry*, 92(14): 10076-10082.
- Manousi, N., Wojnowski, W., Płotka-Wasylka, J., and Samanidou, V. (2023). Blue applicability grade index (BAGI) and software: a new tool for the evaluation of method practicality. *Green Chemistry*, 25(19): 7598-7604.
- 25. Manousi, N., Płotka-Wasylka, J., and Samanidou, V. (2024). Novel sorptive extraction techniques in bioanalysis evaluated by Blue Applicability Grade Index: The paradigm of Fabric phase sorptive extraction and capsule phase microextraction. *TrAC Trends in Analytical Chemistry*, 117586.
- 26. Terzi, M., Theodorou, M., Louloudi, E., Manousi, N., Tzanavaras, P. D., and Zacharis, C. K. (2024). Salicylic acid as a switchable hydrophilicity solvent for the microextraction of the antibiotic amphotericin B from human urine followed by HPLC-UV analysis. *Microchemical Journal*, 199: 110025.
- González-Martín, R., Gutiérrez-Serpa, A., Pino, V., and Sajid, M. (2023). A tool to assess analytical sample preparation procedures: Sample preparation metric of sustainability. *Journal of Chromatography A*, 1707: 464291.
- Utami, M., Wang, S., Musawwa, M. M., Fitri, M., Wijaya, K., Johnravindar, D., ... and Munusamy-Ramanujam, G. (2023). Photocatalytic degradation of naphthol blue from Batik wastewater using

- functionalized TiO2-based composites. *Chemosphere*, 337: 139224.
- 29. Zhang, Q., Zhang, H., Hua, Q., Yuan, C., Wang, X., Zhao, X., and Zheng, B. (2024). Effect on the adsorption performance and mechanism of antibiotics tetracyclines by the magnetic biochar used peanut shells as raw materials. *Materials Research Express*, 11(4): 045508.
- 30. Sandeep, A., and Ravindra, A. V. (2024). Highly efficient peanut shell activated carbon via hydrothermal carbonization and chemical activation for energy storage applications. *Diamond and Related Materials*, 146: 111158.
- 31. Guo, F., Jiang, X., Li, X., Jia, X., Liang, S., and Qian, L. (2020). Synthesis of MgO/Fe₃O₄ nanoparticles embedded activated carbon from biomass for high-efficient adsorption of malachite green. *Materials Chemistry and Physics*, 240: 122240.
- 32. Orduz, A. E., Acebal, C., and Zanini, G. (2021). Activated carbon from peanut shells: 2,4-D desorption kinetics study for application as a green material for analytical purposes. *Journal of Environmental Chemical Engineering*, 9(1), 104601-104601.
- 33. Xu, Y., Liu, Y., Zhan, W., Zhang, D., Liu, Y., Xu, Y., and Wu, Z. (2024). Enhancing CO₂ capture with K₂CO₃-activated carbon derived from peanut shell. *Biomass and Bioenergy*, 183: 107148.
- 34. Nascimento, V. X., Schnorr, C., Lütke, S. F., Da Silva, M. C., Machado Machado, F., Thue, P. S., ... and Dotto, G. L. (2023). Adsorptive features of magnetic activated carbons prepared by a one-step process towards brilliant blue dye. *Molecules*, 28(4): 1821.
- 35. Pebdani, A. A., Shabani, A. M. H., Dadfarnia, S., Talebianpoor, M. S., and Khodadoust, S. (2016). Preconcentration of valsartan by dispersive liquid—liquid microextraction based on solidification of floating organic drop and its determination in urine sample: Central composite design. *Journal of Separation Science*, 39(10): 1935-1944.
- Chen, W. S., Chen, Y. C., and Lee, C. H. (2022).
 Modified activated carbon for copper ion removal from aqueous solution. *Processes*, 10(1): 150.

- 37. Jeirani, Z., Niu, C. H., and Soltan, J. (2017). Adsorption of emerging pollutants on activated carbon. *Reviews in Chemical Engineering*, 33(5): 491-522.
- 38. Saha, N., Das, L., Das, P., Bhowal, A., and Bhattacharjee, C. (2021). Comparative experimental and mathematical analysis on removal of dye using raw rice husk, rice husk charcoal and activated rice husk charcoal: batch, fixed-bed column, and mathematical modeling. *Biomass Conversion and Biorefinery*, 2021: 1-18.
- Khodaie, M., Ghasemi, N., Moradi, B., and Rahimi, M. (2013). Removal of methylene blue from wastewater by adsorption onto ZnCl₂ activated corn husk carbon equilibrium studies. *Journal of Chemistry*, 2013: 383985.
- 40. Tan, I. A. W., Ahmad, A. L., and Hameed, B. H. (2009). Adsorption isotherms, kinetics, thermodynamics and desorption studies of 2, 4, 6-trichlorophenol on oil palm empty fruit bunch-based activated carbon. *Journal of Hazardous Materials*, 164(2-3): 473-482.
- 41. Tamilselvam, S., Loh, S. H., Ariffin, M. M., and Khalik, W. M. A. W. M. (2023). Green and efficient preconcentration of calcium channel blocker drugs in water using effervescence powder in syringe-assisted deep eutectic solvent dispersive liquid-liquid microextraction. *Green Analytical Chemistry*, 7: 100087.
- 42. Wang, T., He, J., Lu, J., Zhou, Y., Wang, Z., and Zhou, Y. (2022). Adsorptive removal of PPCPs from aqueous solution using carbon-based composites: A review. *Chinese Chemical Letters*, 33(8): 3585-3593.
- 43. Islam, M. A., Nazal, M. K., Sajid, M., and Suliman, M. A. (2024). Adsorptive removal of paracetamol from aqueous media: A comprehensive review of adsorbent materials, adsorption mechanisms, recent advancements, and future perspectives. *Journal of Molecular Liquids*, 2024: 123976.
- 44. Rajendran, S., Loh, S. H., Ariffin, M. M., and Khalik, W. M. A. W. M. (2022). Magnetic effervescent tablet-assisted ionic liquid dispersive liquid–liquid microextraction employing the

- response surface method for the preconcentration of basic pharmaceutical drugs: Characterization, method development, and green profile assessment. *Journal of Molecular Liquids*, 367: 120411.
- 45. Vidyadhara, S., Sasidhar, R. L. C., Kumar, B. P., Ramarao, N. T., and Sriharita, N. (2012). Method development and validation for simultaneous estimation of atenolol and nifedipine in pharmaceutical dosage forms by RP-HPLC. *Oriental Journal of Chemistry*, 28(4): 1691.
- 46. Heidari, H., and Limouei-Khosrowshahi, B. (2019). Magnetic solid phase extraction with carbon-coated Fe₃O₄ nanoparticles coupled to HPLC-UV for the simultaneous determination of losartan, carvedilol, and amlodipine besylate in plasma samples. *Journal of Chromatography B*, 1114: 24-30.
- 47. Al-Qaim, F. F., Mussa, Z. H., and Yuzir, A. (2018). Development and validation of a comprehensive solid-phase extraction method followed by LCTOF/MS for the analysis of eighteen pharmaceuticals in influent and effluent of sewage treatment plants. *Analytical and Bioanalytical Chemistry*, 410: 4829-4846.
- 48. Al-Odaini, N. A., Zakaria, M. P., Yaziz, M. I., and Surif, S. (2010). Multi-residue analytical method for human pharmaceuticals and synthetic hormones in river water and sewage effluents by solid-phase extraction and liquid chromatography—tandem mass spectrometry. *Journal of Chromatography A*, 1217(44): 6791-6806.
- Zhao, T., Jiang, W., Zhen, X., Jin, C., Zhang, Y., and Li, H. (2023). Quechers-based approach to the extraction of five calcium channel blockers from plasma determined by UPLC-MS/MS. *Molecules*, 28(2): 671.
- 50. Heidari, H., Razmi, H., and Jouyban, A. (2014). Desirability function approach for the optimization of an in-syringe ultrasound-assisted emulsification-microextraction method for the simultaneous determination of amlodipine and nifedipine in plasma samples. *Journal of Separation Science*, 37(12): 1467-1474.